J. Phycol. **46,** 1138–1151 (2010)

DOI: 10.1111/j.1529-8817.2010.00922.x

STRATEGIES AND RATES OF PHOTOACCLIMATION IN TWO MAJOR SOUTHERN OCEAN PHYTOPLANKTON TAXA: *PHAEOCYSTIS ANTARCTICA* (HAPTOPHYTA) AND *FRAGILARIOPSIS CYLINDRUS* (BACILLARIOPHYCEAE)[1]

Lindsey R. Kropuenske[2], *Matthew M. Mills, Gert L. van Dijken, Anne-Carlijn Alderkamp, Gry Mine Berg*

Department of Environmental Earth System Science, Stanford University, Stanford, California 94305, USA

Dale H. Robinson

Romberg Tiburon Center, San Francisco State University, Tiburon, California 94920, USA

Nicholas A. Welschmeyer

Moss Landing Marine Laboratories, Moss Landing, California 95039, USA

and Kevin R. Arrigo

Department of Environmental Earth System Science, Stanford University, Stanford, California 94305, USA

We investigated rates and mechanisms of photoacclimation in cultures of *Phaeocystis antarctica* G. Karst. and *Fragilariopsis cylindrus* (Grunow) Willi Krieg, phytoplankton taxa that each dominate distinct areas of the Ross Sea, Antarctica. Both *P. antarctica* and *F. cylindrus* acclimated to increases in irradiance by reducing the effective size of the pigment antenna (σPSII) via xanthophyll-cycle activity and reductions in chl. While enhanced photoprotection facilitated increases in specific growth rate and eventually led to higher light-saturated photosynthetic rates (P^{cell}_m) in *P. antarctica*, increases in those variables were much smaller in *F. cylindrus*. In response to a lower irradiance, relaxation of xanthophyll-cycle activity led to an increase in σPSII in both taxa, which occurred much more slowly in *F. cylindrus*. A surprising increase in specific growth rate over the first 36 h of acclimation in *P. antarctica* may have facilitated the significant reductions in P^{cell}_m observed in that taxon. In general, *P. antarctica* acclimated more quickly to changes in irradiance than *F. cylindrus*, exhibited a wider range in photosynthetic rates, but was more susceptible to photoinhibition. This acclimation strategy is consistent with growth in deeply mixed water columns with variations in irradiance that allow time for repair. In contrast, the slower acclimation rates, extensive photoprotection, and low photoinhibition exhibited by *F. cylindrus* suggest that it does not require the same period for repair as *P. antarctica* and is best suited for growth in habitats with relatively uniform irradiance, such as shallow mixed layers or sea ice.

***Key index words: Fragilariopsis cylindrus*; *Phaeocystis antarctica*; photoacclimation; photophysiology; photoprotection; Ross Sea, Antarctica; xanthophyll cycle**

***Abbreviations:* $\bar{a}^*$, mean chl-specific optical absorption cross-section; DD, diadinoxanthin; DT, diatoxanthin; F_v/F_m, maximum photochemical efficiency of PSII; $1/\tau$, turnover rate of the photosynthetic unit; *P-E*, photosynthesis-irradiance; Φ_M, maximum quantum yield of photosynthesis; PSU · cell^{-1}, photosynthetic units per cell; σPSII, effective absorption cross-section of PSII**

Phytoplankton survival in the upper water column requires that cells adjust their photosynthetic machinery in response to changes in their light environment. Phytoplankton have developed various short-term photoprotection mechanisms to tolerate brief and reversible changes in the irradiance field, including state transitions, xanthophyll-cycle heat dissipation, and adjustable RUBISCO activity (MacIntyre et al. 2000, Geider and MacIntyre 2002, Lavaud et al. 2004, Pfannschmidt 2005). However, more significant changes in cellular composition may be required to maintain positive growth if altered conditions persist. On the timescale of several hours to days, the photosynthetic apparatus of phytoplankton cells responds to changes in irradiance via adjustments to the number of photosynthetic units per cell (PSU · cell^{-1}), their effective absorption cross-section (σPSII), or both (Falkowski and LaRoche 1991, Melis et al. 1996, Suggett et al. 2007, Dubinsky and Stambler 2009). Significant variation in light-saturated photosynthetic rates (P_m) in algal cells grown at high compared to low irradiance indicates differences in PSU · cell^{-1} or in their maximum turnover rate ($1/\tau$; P_m = PSU · cell^{-1} * $1/\tau$), which is related to RUBISCO content (Falkowski

[1]Received 4 June 2009. Accepted 26 April 2010.
[2]Author for correspondence: e-mail lindsey.kropuenske@env.ethz.ch.

and Raven 2007). Although variation in light-limited photosynthetic rates (α^*) is influenced by PSU · cell^{-1}, α^* is also controlled by σPSII (α^* = PSU · cell^{-1} * σPSII; Falkowski and Raven 2007). Therefore, significant variation in α^* without changes in P_m generally indicates acclimation primarily via changing σPSII (Dubinsky and Stambler 2009). Because xanthophyll cycling reduces the efficiency of light harvesting by the pigment antenna, thereby reducing σPSII, changes in the ratios of light-harvesting and photoprotective pigments are commonly observed during light transitions (Casper-Lindley and Bjorkman 1998, Moisan et al. 1998, Anning et al. 2000, Leonardos 2008).

The ability and rate with which competing phytoplankton populations acclimate to long-term changes (days to months) in the environment through optimization of cellular components will impact the phytoplankton taxonomic composition in regions that experience strong seasonal changes in environmental variables. In polar regions, in particular, day length, solar angle, winds, ice cover, and water-column structure exhibit large seasonal differences (Arrigo et al. 1998). Melting sea ice or a shoaling of the mixed layer can expose low-light-acclimated phytoplankton to supersaturating irradiance in a period of several hours to a few days in addition to subjecting them to rapid changes in salinity and temperature. Similarly, initiation of strong winds that drive deep water-column mixing and formation of (or advection under) sea ice can subject high-light-acclimated cells to a significantly lower irradiance regime. In the Ross Sea, Antarctica, differences in photoacclimation between major algal taxa could help explain phytoplankton community composition, which tends to follow a regular temporal and spatial pattern.

Briefly, blooms dominated by the haptophyte *P. antarctica* usually develop in spring and summer in the deeply mixed Ross Sea Polynya, while diatom-dominated blooms usually occur during the summer in shallowly mixed, ice-influenced regions (see Mills et al. 2010 for greater detail, Arrigo et al. 1999, Goffart et al. 2000, Wright and van den Enden 2000, Hegseth and von Quillfeldt 2002). Despite the tendency to dominate distinct areas, diatoms and *P. antarctica* both commonly inhabit the sea ice and are ubiquitous throughout the southwestern Ross Sea (DiTullio and Smith 1996, Leventer and Dunbar 1996, Arrigo et al. 2000), suggesting that both taxa have the potential to produce large phytoplankton blooms when environmental conditions are favorable. Although light is often discussed as the major factor controlling phytoplankton production and species distribution, other environmental factors also have been proposed to play a role, particularly on occasions when the sharp gradients in taxonomic composition are not observed (Van Hilst and Smith 2002, Smith et al. 2006, Peloquin and Smith 2007). However, recent work suggests differences between *P. antarctica* and the diatom *F. cylindrus* in photoprotective (Kropuenske et al. 2009) and photosynthetic capacities (Mills et al. 2010) contribute to the observed geographic distributions of phytoplankton in the Ross Sea. Differences between these taxa in photoacclimation rates or strategies could provide an additional dimension to these explanations for light control of phytoplankton dynamics in this region.

Phaeocystis is a cosmopolitan genus with three major species known to produce large blooms in nutrient-rich environments and is thought to be capable of acclimating to a wide range of irradiance (Schoemann et al. 2005). *P. antarctica* in particular has been shown to maintain high photosynthetic rates under low-irradiance conditions by operating at near-maximal quantum efficiency (Cota et al. 1994, Moisan and Mitchell 1999, Mills et al. 2010). In addition, Moisan and Mitchell (1999) demonstrated that the specific growth rate of *P. antarctica* cultures increased with rising irradiance up to 400 μmol photons · m^{-2} · s^{-1} before declining, demonstrating the ability of *P. antarctica* to also grow rapidly at high irradiance. *P. antarctica* also exhibits a wide range in both chl-normalized light-saturated photosynthetic rates (P^*_m) and light-limited rates (α^*) in the field. P^*_m varied from 0.231 to 7.45 mg C · mg^{-1} chl · h^{-1} at various times and locations in *P. antarctica*–dominated waters of the Ross Sea during the 1994 and 1995 growth seasons (Van Hilst and Smith 2002), and from 4.57 to 9.55 mg C · mg^{-1} chl · h^{-1} when *Phaeocystis* was advected under sea ice in 1984 in the Ross Sea (Palmisano et al. 1986). The α^* also varied significantly in both studies, from 0.006 to 0.184 (Van Hilst and Smith 2002) and from 0.0245 to 0.124 mg C · mg^{-1} chl · h^{-1} (μmol photons · m^{-2} · s^{-1})$^{-1}$ (Palmisano et al. 1986). In addition to variation in photosynthetic capacity, *P. antarctica* has been shown to exhibit a significant range in pigment packaging, thylakoid structure, and xanthophyll-cycle pigment content (Moisan et al. 1998, 2006, Kropuenske et al. 2009).

In comparison with *P. antarctica*, smaller differences in light-saturated photosynthetic rates are generally observed in polar diatoms. P^*_m varied from 1.29 to 3.22 mg C · mg^{-1} chl · h^{-1} in diatom-dominated samples from the Ross Sea (Van Hilst and Smith 2002), while α varied between 0.043 and 0.13 mg C · mg^{-1} chl · h^{-1} (μmol photons · m^{-2} · s^{-1})$^{-1}$. In a laboratory comparison of a Ross Sea–isolated diatom, *Pseudonitzschia* sp., and *P. antarctica*, smaller increases in P^*_m were observed in *Pseudonitzschia* sp. (36%) than in *P. antarctica* (104%) when grown at 41 versus 332 μmol photons · m^{-2} · s^{-1} (Van Hilst and Smith 2002). However, α^* declined more with rising irradiance in *Pseudonitzschia* sp. (75%) than in *P. antarctica* (38%), suggesting greater reliance on adjustable pigment antenna size than on changing PSU content in the

polar diatom. Related to this, xanthophyll cycling also has been shown to be critical for avoiding photodamage in polar diatoms, including in cultures of the ecologically important genus *Fragilariopsis* (Mock and Valentin 2004, Kropuenske et al. 2009) and in natural ice-associated diatom assemblages (Robinson et al. 1997, Kudoh et al. 2003, Petrou et al. 2010).

A study investigating photoacclimation in saline Antarctic sea-ice surface ponds determined that diatoms successfully inhabited the high-irradiance surface-ice habitat by employing a strategy that relied on low-light harvesting, high levels of xanthophyll-cycle-mediated energy dissipation, and tolerance of photoinhibitory damage (Robinson et al. 1997). They found that the photosynthetic apparatus of the diatoms cells dominating the algal community (*Navicula glaciei,* >99%) was not acclimated to the high-irradiance conditions (as determined by low values of the photoacclimation parameter, E_k). A similar strategy for survival in high light was proposed to explain the dominance of diatoms in shallow mixed layers of the Ross Sea based on photophysiological laboratory experiments with *F. cylindrus* (Kropuenske et al. 2009). These findings suggest that the photoacclimation strategy of polar diatoms is to adjust σPSII rather than PSU · cell^{-1}.

In this article, we report on a laboratory study that investigated the physiological responses to abrupt changes in light intensity by *P. antarctica* and *F. cylindrus*. Our goal was to determine whether taxonomic differences in rates and strategies for photoacclimation could help explain their observed distributions in the southwestern Ross Sea. In agreement with previous studies demonstrating the wider range over which P^*_m has been shown to vary in *P. antarctica* compared to polar diatoms, and the reliance by polar diatoms on xanthophyll-cycle activity for maintaining photosynthetic performance, we show that *P. antarctica* acclimates to shifts in irradiance with large changes in both photosynthetic capacity (P_m) and α-related changes in light-harvesting efficiency (σPSII), while *F. cylindrus* acclimates primarily by α-related changes.

MATERIALS AND METHODS

Experimental design. Cultures of *P. antarctica* (CCMP #1871) and the diatom *F. cylindrus* (CCMP #1102) were obtained from the Provasoli-Guillard National Center for Culture of Marine Phytoplankton (CCMP; West Boothbay Harbor, ME, USA). *P. antarctica* strain #1871 was collected near Palmer Station in 1991. This particular strain of *P. antarctica* was chosen for light-shift experiments because it grows well in culture and predominately in colonial form, as is often observed in the Ross Sea (Arrigo et al. 1999). *F. cylindrus* strain #1102 was collected in 1979 just east of the Antarctic Peninsula (64.08 S, 48.70 W). We chose *F. cylindrus* as a representative Ross Sea diatom because it (along with similar species of the same genus, e.g., *Fragilariopsis curta*) frequently dominates blooms in the Ross Sea (Leventer and Dunbar 1996, Smith et al. 1996, Gowing et al. 2001, Tortell et al. 2008) and is one of the most abundant diatom species in Antarctic marginal ice zones (Kang and Fryxell 1992). We acquired both nonaxenic cultures from the CCMP in 2003, and stock cultures were maintained under low light (<5 μmol photons · m^{-2} · s^{-1}) and at 2°C in synthetic ocean water (SOW) (Morel et al. 1979) enriched with F/2 macronutrients, micronutrients, and vitamins (Price et al. 1989). Cultures used in these experiments were maintained in exponential growth as semicontinuous cultures under either 5 or 125 μmol photons m^{-2} · s^{-1} for at least 10 generations before experiments were conducted.

Two experiments were conducted in duplicate for each taxon. The first was a high-light shift from 5 to 125 μmol photons · m^{-2} · s^{-1}. The second was a low-light shift from 125 to 5 μmol photons · m^{-2} · s^{-1}. These irradiance conditions were not picked to precisely mimic environmental conditions but because well-acclimated cultures grew exponentially (but at different rates) under both conditions, which were different enough that a significant period of acclimation would be required following a shift and changes in physiology could be observed. Physiological measurements (details follow) were collected at 0, 2, 4, 8, 12, 24, 36, 48, 72, and 96 h after the light shift. Cell abundance was measured at 0, 8, 24, 36, 48, 72, and 96 h. Additional short-term photoprotection measurements were collected 3, 5, 10, 15, 30, and 60 min after each light shift.

Physiological measurements included particulate organic C (POC) concentration, HPLC analysis of pigment concentration, fluorometrically determined chl concentration, photosynthesis versus irradiance (*P-E*) determinations, particulate absorption spectra [$a_p(\lambda)$, m^{-1}], and maximum photochemical efficiency of PSII (Fv/F_m), measured with a pulse-amplitude-modulated (PAM) fluorometer (Water PAM, Heinz Walz GmBH, Effeltrich, Germany). Macronutrient concentrations (nitrate, phosphate, and silicic acid) were monitored for the duration of each experiment to verify that cultures remained nutrient replete. Finally, we estimated the rate of change in several key physiological variables over a 96 h acclimation period independently for each experiment according to both first-order and logistic kinetic models (details follow).

Measurement protocols. *P-E* coefficients, HPLC pigment concentrations, PAM fluorescence measurements, and cell abundance were determined using the methods described in Kropuenske et al. (2009). POC, a_p, quantum yield, and fluorometric chl were measured according to methods described in Arrigo et al. (2010). *P-E* experiments were conducted using 1 h ^{14}C incubations, and coefficients were normalized to (i) cell abundance, (ii) fluorometric chl, and (iii) POC concentrations. Cell-normalized *P-E* time series information is presented in Figures 1 and 3 as it provides better insight into the mechanisms of photoacclimation than chl-, or POC-normalized data (Anning et al. 2000). However, chl- and POC-normalized coefficients at T_0 and T_{96} are included in Table 2 along with rates of change for reference and comparison with other studies. The spectral irradiance of the *P-E* incubator was measured from 300 to 800 nm using a spectroradiometer (Fieldspec, Analytical Spectral Devices Inc., Boulder, CO, USA). Fluorometric chl was used to normalize *P-E* parameters because that data set was deemed to be slightly more reliable than HPLC-determined chl, as fluorometric samples were collected in triplicate and HPLC was collected in duplicate. Despite this, chl concentrations were very similar between fluorometric and HPLC methods. The chl · cell^{-1} was calculated using fluorometric chl to be consistent with fluorometric chl-normalized *P-E* parameters, while diadinoxanthin (DD) and diatoxanthin (DT) · mol^{-1} chl were calculated using HPLC chl from the same sample.

Rate calculations. Using LAB Fit software (Wilton Pereira da Silva, Campina Grande, Brazil), we estimated first-order rate kinetics for changes in physiological parameters using the equation:

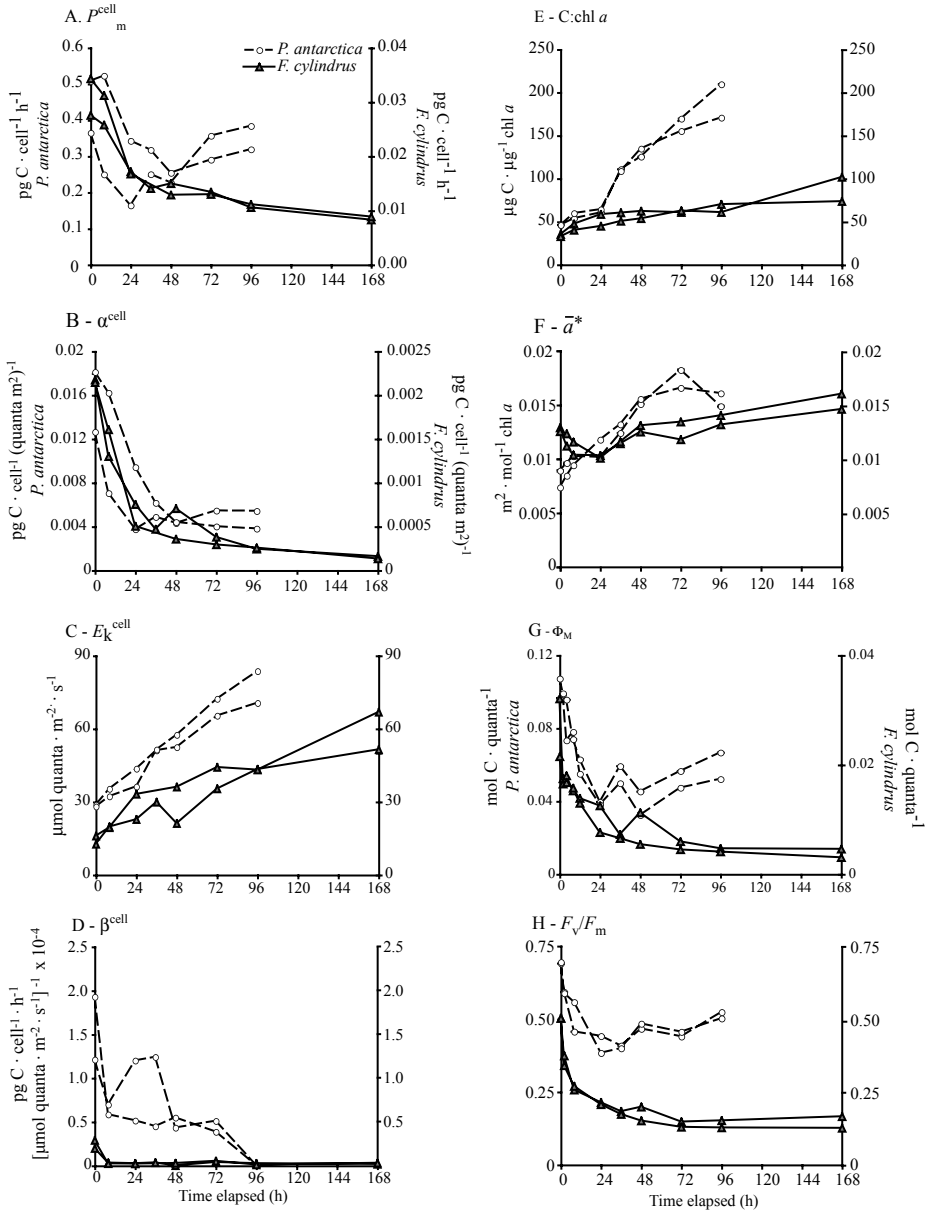

FIG. 1. Photosynthesis-irradiance and physiological parameters: Shift from 5 to 125 µmol photons · m^{-2} · s^{-1}. Changes in the maximum photosynthetic rate (P^{cell}_m) (A), initial slope of the *P-E* curve (α^{cell}) (B), photoacclimation parameter (E_k^{cell}) (C), and photoinhibition parameter (β^{cell}) (D), all normalized to cell abundance, in duplicate cultures of *Phaeocystis antarctica* #1871 (white circles) and *Fragilariopsis cylindrus* #1102 (gray triangles) acclimated to 5 µmol photons · m^{-2} · s^{-1} (T_0) and then shifted to 125 µmol photons · m^{-2} · s^{-1} for 96 h (T_F). Also shown are changes in the C:chl *a* ratio (E), the spectrally averaged optical absorption cross-section ($\bar{a}^*$) (F), quantum yield of photosynthesis (Φ_M) (G), and the maximum quantum yield of chl fluorescence (F_v/F_m) (H). An additional 168 h measurement collected only in *F. cylindrus* cultures is also included.

$$A_T = (A_0 - A_\infty)e^{-kt} + A_\infty \quad (1)$$

where A_T is the variable of interest, A_0 is the value of the variable before the light shift, A_∞ is the steady-state value at the new irradiance, and k is the rate of change in the variable of interest. Many previous studies have used first-order kinetics to describe changes in cellular processes during photoacclimation (Rivkin et al. 1982, Falkowski 1983, 1984, Post et al. 1984, Sukenik et al. 1990). However, it has been observed that although first-order kinetics reasonably describe trends in rapidly changing physiological variables, variables that change more slowly may be modeled better using logistic kinetics (Geider and Platt 1986, Cullen and Lewis 1988). Therefore, we calculated photoacclimation rates using both models. Logistic rate kinetics were estimated according to the equation

$$A_T = \frac{A_\infty}{1 + [(A_\infty - A_0)/A_0)]e^{-kt}} \quad (2)$$

A_0, A_∞, and k were calculated for all variables of interest from the least-squares best fit to the data and calculated independently

for each of the duplicated shift experiments and then averaged for each taxon. If the *P*-value for the rate parameter was <0.10 and A_0 and A_∞ were within 10% of the measured sample value, the curve fit was deemed acceptable and data were presented as bar graphs showing preshift (T_0) and 96 h (T_F) measurements with the rate displayed above. We have noted whenever the *P*-value for the fit of any rate parameter for a given taxon was <0.05 or <0.01 for both treatment duplicates. The kinetic model (first order or logistic) that yielded the highest coefficient of determination (R^2) is presented for each experiment. If neither first-order nor logistic kinetics adequately described the changes in particular variable, no rate is presented and changes are described qualitatively in the text.

RESULTS

Shift from 5 to 125 μmol photons · m^{-2} · s^{-1}. Specific growth rates: Before the shift to 125 μmol photons · m^{-2} · s^{-1}, the growth rates of *P. antarctica* #1871 and *F. cylindrus* #1102 at 5 μmol photons · m^{-2} · s^{-1} were 0.058 and 0.047 d^{-1}, respectively (Table 1). While the specific growth rate increased to 0.076 d^{-1} in *P. antarctica* #1871 cultures following the high-light shift, it did not change significantly in *F. cylindrus* #1102, remaining at 0.047 d^{-1}.

Photosynthetic parameters. P. antarctica*:* Cell-normalized maximum rates of photosynthesis (P^{cell}_m) initially declined in *P. antarctica* #1871 cultures following the shift from low to high irradiance (Fig. 1A). However, between 24 and 48 h, P^{cell}_m began to rise in both cultures, resulting in rates after 96 h that were not significantly less than initial values. The α^{cell} declined precipitously in *P. antarctica*, during the light shift, falling at a rate of 0.104 h^{-1} (Fig. 1B). As a result of changes in P_m and α, E_k^{cell} increased steadily throughout the 96 h experiment (Fig. 1C), at a rate of 0.027 h^{-1}. The photoinhibition parameter, β^{cell}, declined rapidly over the first 8 h of the shift to high light but then remained constant or rose until a second major decline was observed after 72 h (Fig. 1D). A continuous 4-fold rise in the carbon to chl ratio (C:chl) (Fig. 1E) largely explained the increase observed in chl-normalized maximum photosynthetic rates (P^*_m) as well as the decline in C-normalized rates (P^C_m) (Table 1). The α, E_k, and β normalized to chl and POC followed trends during the light shift similar to the cell-normalized parameters.

P. antarctica #1871 exhibited a near doubling in mean chl-specific absorption ($\bar{a}^*$) during the shift to high light (Fig. 1F), with a nearly 3-fold increase in the ratio of absorption in blue relative to red wavelengths (blue:red) (Table 2), suggesting a significant decline in pigment packaging. Despite this increase in $\bar{a}^*$, α (proportional to $\bar{a}^*$ x Φ_M) declined during the light shift. This was explained by a large and rapid drop in Φ_M, which more than offset the rise in $\bar{a}^*$. Eventually, Φ_M reached a plateau after 24 h and then rose again slightly (Fig. 1G). The trend in Φ_M was remarkably similar to that observed in F_v/F_m over the acclimation period (Fig. 1H). Immediately following the shift to high irradiance, F_v/F_m declined rapidly, recovered after approximately 24 h, and then rose slightly thereafter. Φ_M and F_v/F_m both declined with first-order kinetics at rates of 0.177 and 0.193 h^{-1}, respectively, and exhibited values after 96 h that were 57.8% and 65.2% of initial values, respectively. These similarities suggest that electron transport and C fixation were closely tied during the shift to high irradiance.

F. cylindrus*:* In contrast to *P. antarctica*, P^{cell}_m declined by ~65% in *F. cylindrus* #1102 during the 96 h of acclimation to high irradiance (Fig. 1A). Furthermore, P_m was significantly lower in *F. cylindrus* #1102 compared to *P. antarctica* whether normalized to cell abundance, chl, or POC (Table 2) and declined in all cases during acclimation to high irradiance. *F. cylindrus* #1102 exhibited a significant and rapid decline in α and a persistent increase in E_k regardless of the normalization variable (Table 2). For example, α^{cell} declined by nearly 90% and at nearly twice the rate observed in P^{cell}_m (Fig. 1B, Table 2). E_k^{cell} increased approximately 3-fold in both *F. cylindrus* #1102 and *P. antarctica* #1871 over 96 h but was still less than half the ambient irradiance in *F. cylindrus* #1102 after 7 d. The β^{cell} declined faster than any other physiological parameter in *F. cylindrus* #1102, whether normalized to cell abundance, chl, or POC (Fig. 1D, Table 2). In

TABLE 1. Specific growth rates (d^{-1}) calculated from cell abundance measurements collected from acclimated cultures before each light shift (preshift) and during each shift (shift to).

	Preshift 5 μmol photons · m^{-2} · s^{-1}	Shift to 125 μmol photons · m^{-2} · s^{-1}	
Phaeocystis antarctica #1871	0.058* ± 0.004	0.076* ± 0.001	
Fragilariopsis cylindrus #1102	0.047* ± 0.009	0.047* ± 0.013	
	125 μmol photons · m^{-2} · s^{-1}	5 μmol photons · m^{-2} · s^{-1}	
		0–36 h	36–96 h
P. antarctica #1871	0.185* ± 0.001	0.257* ± 0.005	0.095* ± 0.031
		0–96 h	96–168 h
F. cylindrus #1102	0.068* ± 0.027	0.152** ± 0.04	0.042 ± 0.005

Rates were obtained from the fit to an exponential kinetic model. Data presented are mean values for duplicate cultures ± the half variance. The asterisk indicates statistical confidence in the rate estimation at $P < 0.05$. R^2 values for all fits were >0.75.

TABLE 2. Physiological measurements and rates of change (h^{-1}) in *Phaeocystis antarctica* #1871 and *Fragilariopsis cylindrus* #1102 shifted from 5 to 125 µmol photons · m^{-2} · s^{-1} and from 125 to 5 µmol photons · m^{-2} · s^{-1}. Presented are photosynthetic parameters normalized to (i) cell abundance: P^{cell}_m (pg C · $cell^{-1}$ · h^{-1}), α^{cell} [pg C (cell quanta · m^{-2})$^{-1}$], E_k^{cell} (µmol quanta · m^{-2} · s^{-1}), β^{cell} [pg C · $cell^{-1}$ · h^{-1} (µmol quanta · m^{-2} · s^{-1})$^{-1}$]; (ii) chl *a*: P^*_m (µg C · µg chl^{-1} · h^{-1}), α^* [µg C (µg chl quanta · m^{-2})$^{-1}$], E_k^* (µmol quanta · m^{-2} · s^{-1}), β^* [µg C · µg chl · h^{-1} (µmol quanta · m^{-2} · s^{-1})$^{-1}$]; and (iii) particulate organic carbon: P^C_m (h^{-1}), α^C [(quanta · m^{-2})$^{-1}$], E_k^C (µmol quanta · m^{-2} · s^{-1}), β^C [h^{-1} (µmol quanta · m^{-2} · s^{-1})$^{-1}$]. Also presented are mean specific absorption, $\bar{a}^*$ (m^2 · mol^{-1} chl *a*); maximum quantum yield of photosynthesis, Φ_M (mol C · $quanta^{-1}$); maximum quantum yield of fluorescence, F_v/F_m; C:chl *a* (µg:µg); POC · $cell^{-1}$ (pg); chl *a* · $cell^{-1}$ (pg); and ratio of light absorption in blue compared with red wavelengths (blue:red). Mean values are presented for the rate of change, initial values (T_0) and values after 96 h (T_{96}) with the half variation of duplicate cultures shown in parentheses.

5 to 125 µmol quanta · m^{-2} · s^{-1}		*P. antarctica* #1871			*F. cylindrus* #1102	
Parameter	Rate (h^{-1})	T_0	T_{96}	Rate (h^{-1})	T_0	T_{96}
P^{cell}		0.44 (0.10)	0.35 (0.05)	-0.036^{**f} (0.009)	0.031 (0.005)	0.011 (0.0004)
α^{cell_m}	-0.104^{*f} (0.09)	0.015 (0.004)	0.005 (0.001)	-0.060^{**f} (0.001)	21.6 (0.2) × 10^{-4}	2.51 (0.1) × 10^{-4}
E_k^{cell}	0.027^{**1} (0.001)	28.48 (0.55)	77.19 (9.24)	0.019^{**l} (0.003)	14.3 (2.35)	43.28 (0.14)
β^{cell}		1.57 (0.51) × 10^{-4}	5.76 (0.92) × 10^{-8}	-0.353^{*f} (0.029)	24.5 (6.5) × 10^{-6}	1.9 (1.1) × 10^{-6}
P^*_m	0.029^l (0.014)	0.96 (0.15)	2.1 (1.2)	-0.069^{*f} (0.016)	0.184 (0.0003)	0.112 (0.002)
α^*_m	-0.068^{*f} (0.016)	0.039 (0.003)	0.033 (0.016)	-0.070^{*f} (0.014)	0.013 (0.002)	0.003 (0.0001)
E_k^*	0.13^{*l} (0.02)	25.11 (1.94)	71.37 (1.13)	0.023^{**l} (0.002)	14.48 (2.30)	43.79 (1.41)
β^*		5.09 (0.77) × 10^{-4}	3.27 (0.63) × 10^{-4}	-0.712^{**f} (0.206)	14.6 (1.6) × 10^{-5}	3.90 (1.6) × 10^{-5}
P^C_m	-0.091^{*f} (0.014)	0.024 (0.002)	0.011 (0.005)	-0.066^{**f} (0.006)	0.005 (0.001)	0.002 (0.0001)
α^C_m	-0.058^{**f} (0.004)	7.7 (0.46) × 10^{-4}	1.6 (0.67) × 10^{-4}	-0.074^{*f} (0.020)	3.6 (0.07) × 10^{-4}	0.31 (0.09) × 10^{-4}
E_k^C	0.025^{*l} (0.003)	30.65 (0.75)	71.85 (1.44)	0.027^{**l} (0.009)	14.32 (2.34)	51.74 (11.94)
β^C	−0.400 (0.322)	11.8 (4.1) × 10^{-6}	2.23 (0.15) × 10^{-6}	-0.635^{**f} (0.04)	10.3 (10.0) × 10^{-7}	3.3 (0.99) × 10^{-7}
$\bar{a}*$	0.041^{*l} (0.010)	0.008 (0.001)	0.015 (0.001)		0.127 (0.0002)	0.0136 (0.001)
Φ_M	-0.177^{*f} (0.012)	0.102 (0.006)	0.059 (0.010)	-0.098^{*f} (0.060)	0.027 (0.008)	0.004 (0.001)
F_v/F_m	-0.193^{*f} (0.094)	0.69 (0.003)	0.45 (0.011)	0.099^{**f} (0.029)	0.50 (0.0001)	0.14 (0.017)
C:chl *a*	0.034^{**l} (0.003)	46.24 (0.06)	190.3 (27.4)	0.028^{*l} (0.030)	34.02 (1.73)	65.44 (6.62)
POC · $cell^{-1}$	0.012^{*l} (0.001)	16.0 (0.31)	28.8 (11.3)		7.49 (0.08)	6.49 (0.1)
Chl *a* · $cell^{-1}$	0.027^{*l} (0.007)	0.32 (0.03)	0.13 (0.005)	-0.014^{*f} (0.0001)	0.19 (0.06)	0.095 (0.002)
Blue:red	0.024^l (0.008)	1.60 (0.02)	4.55 (0.54)	0.015^l (0.011)	1.34 (0.05)	1.53 (0.10)

125 to 5 µmol quanta · m^{-2} · s^{-1}		*P. antarctica* #1871			*F. cylindrus* #1102	
Parameter	Rate (h^{-1})	T_0	T_{96}	Rate (h^{-1})	T_0	T_{96}
P^{cell}	-0.054^{*f} (0.058)	0.78 (0.01)	0.33 (0.05)	0.081^l (0.024)	0.041 (0.0001)	0.055 (0.005)
α^{cell_m}	-0.056^{*f} (0.037)	0.012 (0.001)	0.007 (0.002)	0.028^{*f} (0.007)	9.84 (0.17) × 10^{-4}	31.4 (2.7) × 10^{-4}
E_k^{cell}	-0.005^{*f} (0.0006)	66.74 (7.00)	51.15 (4.35)	-0.046^{*f} (0.010)	41.4 (0.66)	24.2 (1.50)
β^{cell}		3.25 (2.17) × 10^{-5}	39.4 (3.8) × 10^{-5}	0.024^l (0.012)	1.0 (0.14) × 10^{-5}	1.6 (0.11) × 10^{-5}
P^*_m	-0.269^f (0.193)	3.29 (0.035)	3.15 (0.20)		1.04 (0.10)	0.88 (0.13)
α^*_m		0.050 (0.006)	0.062 (0.009)	0.149^{*l} (0.043)	0.024 (0.001)	0.037 (0.008)
E_k^*	-0.129^{*f} (0.064)	66.60 (6.87)	51.21 (4.26)	-0.44^{*f} (0.09)	42.9 (2.8)	24.2 (1.5)
β^*	0.167^{*l} (0.046)	0.04 (0.05) × 10^{-3}	2.4 (0.34) × 10^{-4}	0.009^l (0.006)	2.86 (1.0) × 10^{-4}	5.4 (0.05) × 10^{-4}
P^C_m	0.026^{*l} (0.004)	0.024 (0.002)	0.038 (0.001)	0.103^{*l} (0.01)	0.012 (0.0004)	0.018 (0.002)
α^C_m	0.029^{*l} (0.005)	2.7 (0.5) × 10^{-4}	8.0 (0.7) × 10^{-4}	0.131^{*l} (0.013)	2.7 (0.08) × 10^{-4}	7.4 (0.24) × 10^{-4}
E_k^C	-0.154^{*f} (0.007)	64.85 (4.02)	47.35 (3.27)	-0.44^{*f} (0.09)	42.9 (2.82)	24.2 (1.46)
β^C	0.134^{*l} (0.051)	0.095 (0.08) × 10^{-5}	4.9 (1.6) × 10^{-5}	0.076^l (0.005)	0.31 (0.09) × 10^{-5}	0.53 (0.03) × 10^{-5}
$\bar{a}*$		0.013 (0.002)	0.011 (0.0004)	0.44^f (0.18)	0.015 (0.001)	0.011 (0.002)
Φ_M		0.084 (0.014)	0.117 (0.009)	0.140^{*l} (0.002)	0.038 (0.005)	0.100 (0.007)
F_v/F_m	0.045^{*l} (0.011)	0.59 (0.01)	0.67 (0.001)	0.44^{**l} (0.12)	0.41 (0.01)	0.65 (0.01)
C:chl *a*	-0.035^{*f} (0.006)	147.2 (4.20)	78.06 (2.84)	-0.048^{*f} (0.020)	90.6 (5.3)	50.1 (11.8)
POC · $cell^{-1}$	-0.157^{*f} (0.123)	26.1 (1.6)	9.22 (0.29)	-0.16^{**f} (0.12)	4.77 (0.32)	1.04 (0.20)
Chl *a* · $cell^{-1}$	-0.092^{*f} (0.016)	0.19 (0.04)	0.12 (0.004)	0.019^{*l} (0.013)	0.035 (0.0004)	0.071 (0.002)
Blue:red	-0.213^f (0.029)	7.22 (0.35)	3.95 (0.30)	-0.016^{*f} (0.001)	1.90 (0.04)	1.54 (0.09)

The superscripts *l* and *f* associated with rate information indicate whether a logistic or first-order kinetic model was used to calculate the rate of change, respectively. * and ** indicate statistical confidence in the rate at $P < 0.05$ and $P < 0.01$, respectively. If a persistent trend was not observed and rates of change could not be estimated adequately with either model, no rate estimate is presented.

contrast to the significant rise in POC · cell^{-1} in *P. antarctica*, POC · cell^{-1} declined slightly in *F. cylindrus* #1102, resulting in smaller changes in C:chl, which still rose significantly (Fig. 1E) due to a nearly 50% decline in chl · cell^{-1} (Table 2).

Trends in $\bar{a}^*$ changed with time in *F. cylindrus* #1102 following the shift to high irradiance (Fig. 1F). $\bar{a}^*$ declined over the first 24 h but then rose slowly to attain values after 96 h that were significantly higher than initial values. Pigment packaging declined slightly in *F. cylindrus* #1102 (Table 2), but blue:red did not increase to nearly the same extent as was observed in *P. antarctica*. As with *P. antarctica*, Φ_M exhibited a large and rapid decline according to first-order kinetics (Fig. 1G, Table 2). The initial declines in $\bar{a}^*$ and Φ_M in *F. cylindrus* #1102 explain well the steep drop in α^{cell} that occurred over the first 24 h of the high-light shift. Despite similar rates of decline, F_v/F_m declined by less than Φ_M (72% and 86%, respectively, after 96 h, Fig. 1H, Table 2), suggesting that electron transport exceeded C fixation to a small degree during high-light acclimation in *F. cylindrus* #1102.

Chl and xanthophyll-cycle pigments. P. antarctica*:* Transfer of *P. antarctica* #1871 from 5 to 125 μmol photons · m^{-2} · s^{-1} resulted in substantial changes in chl as well as in short- and long-term xanthophyll-cycle activity. *P. antarctica* #1871 exhibited significant declines in chl · cell^{-1} (Fig. 2A) that took place faster than in *F. cylindrus*. Total xanthophyll-cycle pigment per cell (DD + DT · cell^{-1}) declined in concert with chl over the first 36 h of the shift to high irradiance but increased thereafter (data not shown). However, the balance between light harvesting and photoprotection within the photosynthetic apparatus is best assessed by normalizing the concentrations of xanthophyll-cycle pigments to that of chl. The DD · mol^{-1} chl declined immediately in *P. antarctica* #1871 and by almost 50% over the 96 h acclimation period (Fig. 2B) as demand for de-epoxidated xanthophyll-cycle pigment (DT) increased. While the rate of DD decline was 2.24 h^{-1} and followed first-order rate kinetics when calculated over the entire acclimation period, a second significant first-order relationship was observed within the first 2 h, with DD · mol^{-1} chl declining at the faster rate of 4.75 h^{-1}.

Surprisingly, DT · mol^{-1} chl followed the opposite trend in *P. antarctica* #1871, with a higher rate of change measured over the 96 h acclimation period (0.49 h^{-1}) compared with the rate of the first 2 h (0.24 h^{-1}). This trend was likely due to substantial de novo DT synthesis after the first 2 h. Overall, DT · mol^{-1} chl increased ~5-fold in *P. antarctica* #1871 (Fig. 2C), with the more modest decrease in DD · mol^{-1} chl suggesting that either DT was synthesized directly or rapidly converted from DD. The declines in DD and increases in DT resulted in a dramatic rise in the xanthophyll-cycle de-epoxidation ratio (DT:[DD + DT]), which rose from 0.11 to 0.62 (Fig. 2D).

F. cylindrus*:* As in *P. antarctica*, chl · cell^{-1} declined significantly when *F. cylindrus* #1102 was shifted to high irradiance (Fig. 2A). DD+DT · cell^{-1} also declined over the first 36 h of acclimation before increasing gradually thereafter (data not shown). However, xanthophyll-cycle pigment concentrations normalized to chl reveal the strong reliance on xanthophyll-cycle activity by *F. cylindrus* during acclimation to high irradiance. DD · mol^{-1} chl declined by nearly 60% in *F. cylindrus* #1102 (Fig. 2B), with rates of decline calculated over the first 2 h that were even larger than in *P. antarctica* (16 h^{-1}). However, rates of decline in DD · mol^{-1} chl were lower in *F. cylindrus* #1102 than in *P. antarctica* #1871 when calculated over the 96 h experiment (0.388 h^{-1}). Exceeding changes in DD due to de novo synthesis, DT · mol^{-1} chl increased

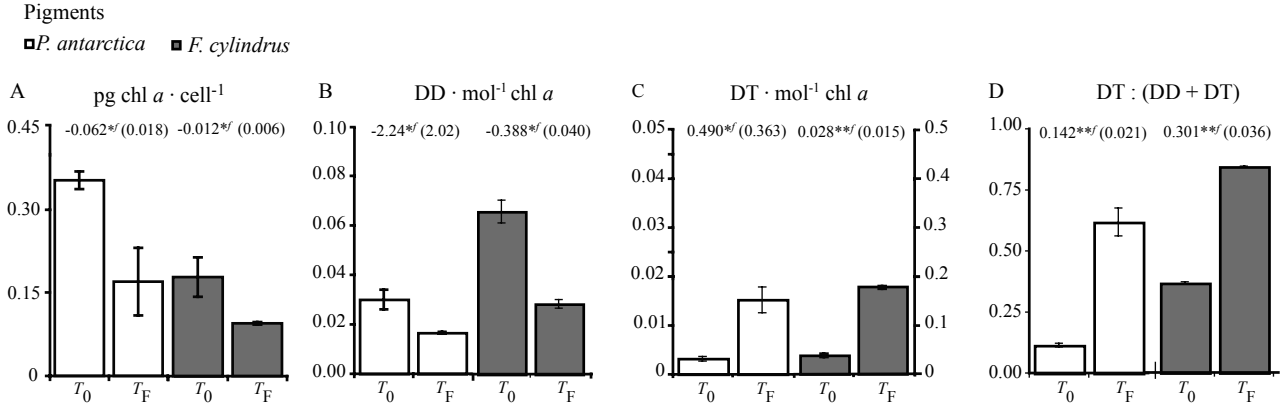

FIG. 2. Changes in chl and xanthophyll-cycle pigments: Shift from 5 to 125 μmol photons · m^{-2} · s^{-1}. Changes in cellular concentrations of chl (pg) (A), chl-normalized concentrations of diadinoxanthin (DD) (B) and diatoxanthin (DT) (C), and the xanthophyll-cycle pigment de-epoxidation ratio DT:(DD + DT) (D) in cultures of *Phaeocystis antarctica* #1871 and *Fragilariopsis cylindrus* #1102 acclimated to 5 μmol photons · m^{-2} · s^{-1} (T_0) and then shifted to 125 μmol photons · m^{-2} · s^{-1} for 96 h (T_F). The numbers above the data indicate the mean and half variation of the rate of change in each variable for duplicate experiments. * and ** indicate the confidence of the rate parameter, when $P < 0.05$ and <0.001, respectively. *f* and *l* indicate a first-order or logistic curve fit, respectively.

from 0.04 ± 0.003 to 0.18 ± 0.003 over 96 h of acclimation to high irradiance, tripling between 2 and 96 h. However, DT · mol^{-1} chl increased much more rapidly (6.73 h^{-1}) during the first 2 h of the light shift than when calculated over the entire experiment (0.028 h^{-1}) (Fig. 2C). The value of DT:(DD + DT) increased from a preshift value of 0.37 to 0.70 after 2 h at a rate of 16 h^{-1}, increasing to 0.85 after 96 h at an overall rate of 0.301 h^{-1} (Fig. 2D).

In the short-term (first 2 h), changes in xanthophyll-cycle pigment concentrations were more rapid in *F. cylindrus* #1102 than in *P. antarctica* #1871, indicating a faster photoprotective response. However, when calculated over the course of the entire experiment, the rates of change in DD and DT · mol^{-1} chl were higher in *P. antarctica* #1871, illustrating its need for xanthophyll-cycle photoprotection when exposed to high irradiance for extended periods and its ability to synthesize relatively large concentrations when necessary. It is important to note, however, that although de-epoxidation ratios and rates of pigment production over the course of the light shift were similar for *P. antarctica* #1871 and *F. cylindrus* #1102, concentrations of DD · mol^{-1} chl and DT · mol^{-1} chl in *F. cylindrus* #1102 cultures were ~2- and 10-fold higher, respectively, than in *P. antarctica* #1871 cultures.

Shift from 125 to 5 μmol photons · m^{-2} · s^{-1}. Specific growth rates: Prior to the shift from 125 to 5 μmol photons · m^{-2} · s^{-1}, *P. antarctica* #1871 grew with a cell-specific growth rate of 0.185 d^{-1} (Table 1). *F. cylindrus* #1102 grew significantly slower, at 0.068 d^{-1}, although faster than when it was acclimated to 5 μmol photons · m^{-2} · s^{-1}. Initially, specific growth rates increased upon transition to low irradiance in both taxa, by nearly 40% in *P. antarctica* #1871 and by >100% in *F. cylindrus* #1102, suggesting that 125 μmol photons · m^{-2} · s^{-1} exceeded the optimal growth irradiance in both taxa (under continuous light conditions). Rapid rates of cell division were observed in *P. antarctica* #1871 until ~36 h, at which point the exponential growth rate slowed significantly (Table 1). However, it remained higher than that observed in cells fully acclimated to 5 μmol photons · m^{-2} · s^{-1} for the duration of the 96 h observation period. In *F. cylindrus* #1102, growth rates were elevated above preshift values for the first 96 h of acclimation to low irradiance. Specific growth rates appeared to slow between 96 and 168 h, but with only two data points available to make the calculation in each culture, the significance of the decline could not be confirmed.

Photosynthetic parameters. P. antarctica*:* P^{cell}_m declined by >50% in *P. antarctica* #1871 after being shifted from 125 to 5 μmol photons · m^{-2} · s^{-1} (Fig. 3A), and after 36 h, rates were not significantly different from those observed in cells fully acclimated to 5 μmol photons · m^{-2} · s^{-1}. Surprisingly, α^{cell} also declined by slightly less than 50% (Fig. 3B). Declining trends in both P^{cell}_m and α^{cell} were likely affected by the initially rapid increase in cell abundance (Table 1) observed upon transition to low irradiance. Both α^{cell} and P^{cell}_m stopped declining after 36 h, when growth rates slowed. The values of α^{cell} and P^{cell}_m changed at similar rates and with first-order kinetics (Table 2), resulting in a decline in E_k^{cell} (Fig. 3C, Table 2) that occurred much more slowly and was significantly smaller than that observed during the shift from low to high irradiance. Immediately following the shift to low irradiance, β^{cell} increased rapidly, then reached a plateau or declined after ~36 h (Fig. 3D). A very large, consistent decline was observed in C:chl over the 96 h experiment (Fig. 3D), explaining the declines observed in P^{*}_m and increases in P^{C}_m (Table 2). Increases were observed in both α^{*} and α^{C}, however, in contrast with α^{cell}. Despite these differences, E_k was similar regardless of the normalization variable. The β increased significantly in all cases, although a smooth trend was observed only when normalized to chl (Table 2).

The $\bar{a}^*$ declined rapidly in *P. antarctica* #1871 upon transfer to low irradiance (Fig. 3F) before climbing more slowly after ~8 h. Changes in mean absorption were accompanied by a significant decline in blue:red, implying enhanced pigment packaging. However, after 96 h of acclimation to 5 μmol photons · m^{-2} · s^{-1}, blue:red was still significantly higher than that observed in cultures fully acclimated to that irradiance (3.95 vs. 1.60, respectively). The initial declines in $\bar{a}^*$ appear to have driven the early declines in α^{cell}, as Φ_M increased significantly and rapidly over the first 24 h of exposure to low irradiance in *P. antarctica* #1871 (Fig. 3G). However, after 24 h, Φ_M began to decline again, probably accounting for the continued decline in α^{cell}, as $\bar{a}^*$ had already begun to increase. After a gradual decline, Φ_M began to rise once again after 72 h, ultimately increasing by 39% above T_0 values and reaching levels observed in cells fully acclimated to 5 μmol photons · m^{-2} · s^{-1}. F_v/F_m did not increase by as much as Φ_M (only 13.6%, Fig. 3H), although both F_v/F_m and Φ_M approached their theoretical maximum by the end of 96 h.

F. cylindrus*:* After an initial delay, P^{cell}_m rose in *F. cylindrus* #1102 (Fig. 3A), ultimately increasing by 34% above T_0 values (Table 2). The increase in α^{cell} was even larger (>3-fold, Fig. 3B), although it was relatively slow. The E_k^{cell} declined significantly (Fig. 3C) and by a larger fraction than was observed in *P. antarctica*. The β^{cell} slowly increased by ~60% over the 168 h experiment (Fig. 3D). A significant decline in C:chl (Fig. 3E) resulted in an overall decline in P^{*}_m, with a concurrent increase in P^{C}_m. The α increased and E_k declined regardless of the normalization variable (Table 2). A large drop in C:chl resulted from a significant decline in POC · $cell^{-1}$ (80%) and a doubling in chl · $cell^{-1}$.

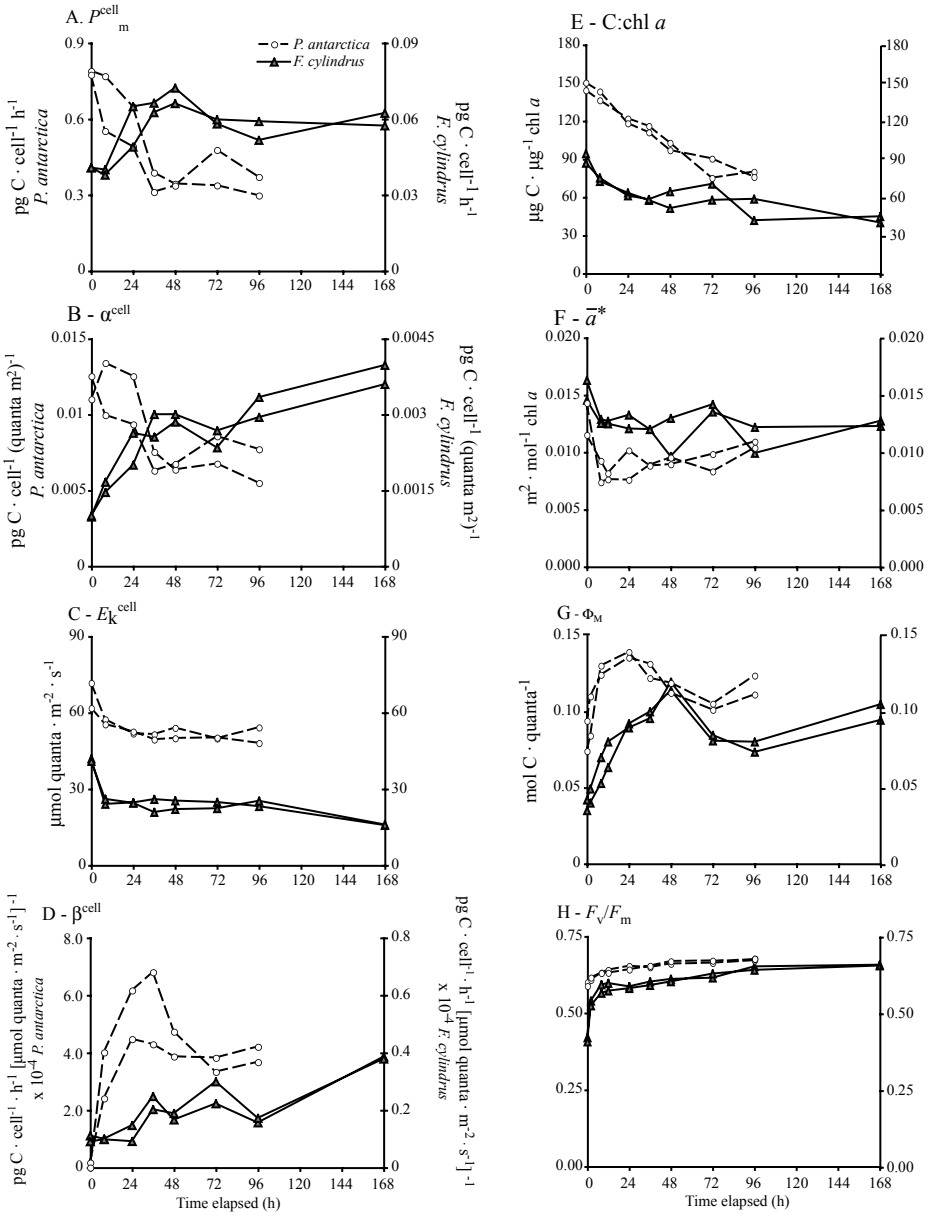

FIG. 3. Photosynthesis-irradiance and physiological parameters: Shift from 125 to 5 µmol photons · m^{-2} · s^{-1}. Changes in the maximum photosynthetic rate (P^{cell}_m) (A), initial slope of the *P-E* curve (α^{cell}) (B), photoacclimation parameter (E_k^{cell}) (C), and photoinhibition parameter (β^{cell}) (D), all normalized to cell abundance, in duplicate cultures of *Phaeocystis antarctica* #1871 (white circles) and *Fragilariopsis cylindrus* #1102 (gray triangles) acclimated to 125 µmol photons · m^{-2} · s^{-1} (T_0) and then shifted to 5 µmol photons · m^{-2} · s^{-1} for 96 h (T_F). Also shown are changes in the C:chl *a* ratio (E), the spectrally averaged optical absorption cross-section ($\bar{a}^*$) (F), quantum yield of photosynthesis (Φ_M) (G), and the maximum quantum yield of chl fluorescence (F_v/F_m) (H). An additional 168 h measurement collected only in *F. cylindrus* cultures is also included.

Reflecting the increase in chl · cell^{-1}, $\bar{a}^*$ declined following the transition to low irradiance (Fig. 3F). This was accompanied by a small but significant decline in blue:red, suggesting increased pigment packaging (Table 2). The decline in $\bar{a}^*$ was offset by a substantial increase in Φ_M, which accounted for the rise in α^{cell}. Φ_M increased continuously for the first 48 h of exposure to low irradiance before declining somewhat and then rising again at ~96 h. Over the course of the experiment, Φ_M increased in *F. cylindrus* #1102 by > 160%. Although F_v/F_m increased by only 58% (Fig. 3H), it was much faster (Table 2), illustrating a rapid recovery in functional reaction centers and the capacity for electron transport.

Chlorophyll and xanthophyll-cycle pigments. P. antarctica*:* Surprisingly, chl · cell^{-1} declined in *P. antarctica* #1871 during acclimation to low irradiance (Fig. 4A). This was a result of an initial increase in the cell-specific growth rate after the transition to low irradiance that exceeded the rate of chl increase. However, POC · cell^{-1} dropped by a

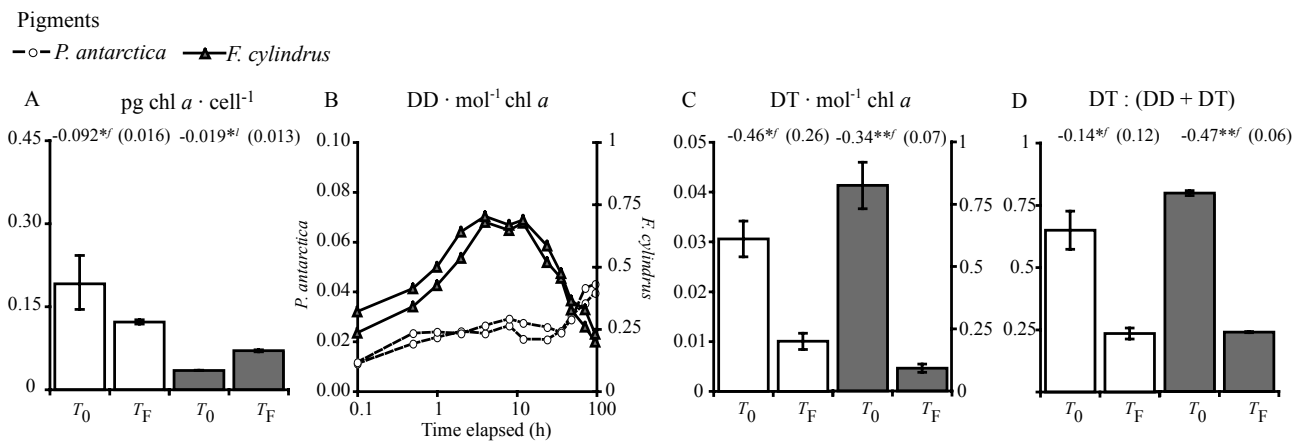

FIG. 4. Changes in chl and xanthophyll-cycle pigments: Shift from 125 to 5 μmol photons · m^{-2} · s^{-1}. Changes in cellular concentrations of chl (pg) (A), chl-normalized concentrations of diadinoxanthin (DD) (B) and diatoxanthin (DT) (C), and the xanthophyll-cycle pigment de-epoxidation ratio DT:(DD + DT) (D) in cultures of *Phaeocystis antarctica* #1871 and *Fragilariopsis cylindrus* #1102 acclimated to 125 μmol photons · m^{-2} · s^{-1} (T_0) and then shifted to 5 μmol photons · m^{-2} · s^{-1} for 96 h (T_F). T_0 and T_F values are presented unless data did not fit a first-order or logistic model with $R^2 > 0.85$; in that case, change in that variable over time is presented. The numbers above the data indicate the mean and half variation of the rate of change in each variable for duplicate experiments. * and ** indicate the confidence of the rate parameter, when $P < 0.05$ and <0.001, respectively. *f* and *l* indicate a first-order or logistic curve fit, respectively.

greater amount and more rapidly than chl · $cell^{-1}$ (Table 2), resulting in a decline in C:chl. As with chl · $cell^{-1}$, DD + DT · $cell^{-1}$ dropped sharply within the first 36 h of the shift to low irradiance (data not shown), corresponding to increased cell abundance. Concentrations began to rise slowly thereafter but did not reach preshift concentrations. More importantly, analysis of the xanthophyll-cycle pigments relative to chl reveals a notable decrease in xanthophyll-cycle activity. The DD · mol^{-1} chl approximately doubled (~0.01–0.02) within the first 30 min of the shift to low irradiance, presumably as DT present before the light shift was expoxidated to form DD (Fig. 4B). Concentrations continued to rise gradually until ~48 h when DD · mol^{-1} chl began to rise more sharply, approximately doubling again by the end of the experiment. The DT · mol^{-1} chl declined uniformly but very rapidly (at a rate of 0.46 h^{-1}), from 0.031 ± 0.003 to 0.01 ± 0.007 mol DT · mol^{-1} chl (Fig. 4C). Consistent with declining xanthophyll-cycle activity, DT:(DD + DT) declined by nearly 70%, at a rate of 0.15 h^{-1} (Fig. 4D), which was virtually identical to the rate of increase during the shift to high light (0.142 h^{-1}).

F. cylindrus*:* In contrast to *P. antarctica*, *F. cylindrus* #1102 exhibited a doubling in chl · $cell^{-1}$ during acclimation to low irradiance (Fig. 4A, Table 2). However, cellular chl concentrations after 96 h were still significantly less than concentrations in cells fully acclimated to 5 μmol photons · m^{-2} · s^{-1} (T_0 shift up, Table 2). Trends in cell-normalized DD and DT concentrations were similar to the chl-normalized trends, with total xanthophyll-cycle pigment per cell remaining fairly constant over the first 4 h of acclimation to low irradiance and then decreasing approximately linearly, in concert with increasing cell number (data not shown). Analysis of chl-normalized xanthophyll-cycle pigments reveals that a substantial decline in xanthophyll-cycle activity was a prominent feature of acclimation to low irradiance in *F. cylindrus* #1102. The DD · mol^{-1} chl increased rapidly within the first 4 h of the shift to low irradiance (Fig. 4B), from 0.28 ± 0.06 mol^{-1} chl to a maximum of 0.69 ± 0.016 mol^{-1} chl (Fig. 5B) as DT was epoxidated to form DD. This initial increase in DD · mol^{-1} chl occurred over a significantly longer period in *F. cylindrus* #1102 (4 h) than it did in *P. antarctica* #1871 (15 min), revealing strong differences between taxa in their utilization of xanthophyll-cycle photoprotection under high-light conditions. DD concentrations declined steadily after 12 h, eventually dropping below preshift concentrations after 96 h (0.21 ± 0.02). DT concentrations decreased rapidly from 0.83 ± 0.09 to 0.34 ± 0.001 mol^{-1} chl after 4 h (Fig. 4C), mirroring the increase in DD observed over the same period. After 96 h, DT concentrations had declined to 0.09 ± 0.02 mol^{-1} chl, only 28% of their initial value. Furthermore, DT:(DD + DT) dropped from 0.80 ± 0.01 to 0.24 ± 0.002, at a rate of 0.47 h^{-1} (Fig. 4D), faster than the rate at which DT:(DD + DT) increased during the shift to high irradiance and similar to the rate of increase in F_v/F_m (Table 2).

DISCUSSION

We observed significant changes in both photosynthetic capacity and light-harvesting efficiency in *P. antarctica* #1871 cultures acclimated to low and high irradiance. Although $P^{cell}{}_m$ was much higher in cells fully acclimated to the high-light treatment, $P^{cell}{}_m$ declined initially following transfer from low to high light, likely due to photoinhibitory damage

incurred before enough xanthophyll-cycle pigment could be synthesized so that the rate of photorepair could exceed the rate of photodamage. The rapid parallel declines in the quantum yield of photosynthesis (Φ_M) and fluorescence (F_v/F_m) imply that photodamage was significant after the transition to saturating irradiance, with damaged photosystems reducing the flow of electrons to photochemistry. This damage also contributed to the large drop in α^{cell}. F_v/F_m, Φ_M, and $P^{cell}{}_m$ all began to rise in *P. antarctica* #1871 at ~36–48 h, by which time DT · mol^{-1} chl had increased ~10-fold. Although 96 h was not sufficient to observe full acclimation of *P. antarctica* #1871 to 125 μmol photons · $m^{-2} \cdot s^{-1}$, it appears that synthesis of additional xanthophyll-cycle pigments, along with reductions in chl, reduced the effective size of the pigment antenna (σPSII) and facilitated the transition to high irradiance. This step eventually allowed for repair of damaged photosystems, and for an increase in the cell-specific growth rate and additional photosynthetic capacity, as evidenced by higher $P^{cell}{}_m$ and specific growth rates in cells fully acclimated to 125 μmol photons · $m^{-2} \cdot s^{-1}$. The additional photosynthetic capacity most likely resulted from an increase in $1/\tau$ as opposed to an increase in PSU · $cell^{-1}$, which generally declines with rising irradiance if it changes significantly (Falkowski and Raven 2007, Dubinsky and Stambler 2009). A 14% reduction in F_v/F_m in cells acclimated to 125 versus 5 μmol photons · $m^{-2} \cdot s^{-1}$ suggests that PSU · $cell^{-1}$ may have declined slightly in *P. antarctica* #1871.

Upon the shift to high irradiance, *P. antarctica* #1871 was able to utilize higher irradiance and grow more quickly once it had sufficiently reduced σPSII. However, when transferred from 125 to 5 μmol photons · $m^{-2} \cdot s^{-1}$, the cell-specific growth rate did not decline as expected but rather increased over the first 36 h of the acclimation period before declining. Due to the rapid rate of cell division, $P^{cell}{}_m$ declined for the first 36 h to just below the rate exhibited by cells fully acclimated to 5 μmol photons · $m^{-2} \cdot s^{-1}$ (Table 2). Surprisingly, α^{cell} also declined despite a significant reduction in xanthophyll pigment de-epoxidation and large increases in Φ_M, which suggest a significant rise in σPSII. Both $P^{cell}{}_m$ and α^{cell} stopped declining after 36 h, coinciding with reduced rates of cell division. Presumably, cell-specific growth rates would continue to slow to the significantly lower values exhibited by cells fully acclimated to 5 μmol photons · $m^{-2} \cdot s^{-1}$. As cells generally do not degrade molecules during acclimation (Falkowski 1984, Post et al. 1984), maintaining high rates of cell division might serve to ''dilute'' photosynthetic capacity, thereby facilitating acclimation to low irradiance. Although low chl · $cell^{-1}$ and α^{cell} suggest that *P. antarctica* was not well acclimated to 5 μmol photons · $m^{-2} \cdot s^{-1}$ after 96 h, by that time, $P^{cell}{}_m$, $\bar{a}^*$, Φ_M, and F_v/F_m had all attained values similar to those in cells fully acclimated to 5 μmol photons · $m^{-2} \cdot s^{-1}$. This finding suggests that *P. antarctica* #1871 employed a strategy for acclimating to low irradiance that utilized rapid cell division to quickly reduce photosynthetic capacity, most likely by reducing RUBISCO-related $1/\tau$, as PSU · $cell^{-1}$ tends to increase with falling irradiance if it changes at all. σPSII changed more slowly than changes in photosynthetic capacity during low-light acclimation, in contrast to the rapid changes in σPSII that facilitated slower changes in photosynthetic capacity during high-light acclimation.

Our findings suggest that *P. antarctica* #1871 acclimates to changes in irradiance by adjusting both the effective size of its pigment antenna (σPSII) and photosynthetic capacity (PSU · $cell^{-1}$ or $1/\tau$). Although this was determined in just one *P. antarctica* strain, photoacclimation in this manner is consistent with studies in other haptophytes. Photoacclimation to high irradiance via a decrease in σPSII has previously been documented as the primary photoacclimation mechanism in the haptophyte *Isochrysis galbana* (Dubinsky et al. 1986). Decreasing σPSII also was shown to be important in the haptophyte *Emiliania huxleyi.* σPSII declined by 34% and 14% between 25 and 600 μmol photons · $m^{-2} \cdot s^{-1}$ in two different strains of *E. huxleyi,* one of which preferentially changed σPSII over photosystem number, while the other changed both (Suggett et al. 2007).

The physiological data reported in this study are also consistent with data from the field and other laboratory studies. The *P-E* coefficients in *P. antarctica* were well within the range of those measured in *P. antarctica*–dominated regions of the Ross Sea (Van Hilst and Smith 2002), but slightly higher than values measured in cultures presented in the same study. However, *P. antarctica* was grown at 2°C in our study, rather than 0°C. Specific growth rates, chl · $cell^{-1}$, Φ_M, $\bar{a}^*$, xanthophyll-cycle pigment concentrations, and de-epoxidation rates presented here also were consistent with data reported in Moisan et al. (1998) and Moisan and Mitchell (1999).

In *F. cylindrus* #1102, changes in response to irradiance were significantly larger in α^{cell} than in $P^{cell}{}_m$, with xanthophyll-cycle activity mediating large changes in the efficiency of light absorption and maintaining strong control over photochemistry during photoacclimation. $P^{cell}{}_m$ was 37% higher, and α^{cell} 55% lower in cells fully acclimated to 125 μmol photons · $m^{-2} \cdot s^{-1}$ than those acclimated to 5 μmol photons · $m^{-2} \cdot s^{-1}$ (Table 2). During the shift up in irradiance, xanthophyll-cycle activity was immediately initiated by *F. cylindrus* #1102 and maintained at high levels for the duration of the experiment. Unlike in *P. antarctica*, a large pool of xanthophyll-cycle pigment was present before the shift to high light in *F. cylindrus* #1102, resulting in significantly lower β^{cell} at T_0. Although some DT was synthesized de novo by in *F. cylindrus* #1102, and β^{cell} declined during high-light acclimation, the large initial concentrations of DT significantly

reduced the efficiency of light absorption, producing a steep decline in Φ_M (Fig. 1G). This, in turn, drove the decline in α^{cell} (Fig. 1B), which dropped more rapidly than P^{cell}_m. However, the declines observed in P^{cell}_m most likely indicated a decline in functional PSU · cell^{-1}, which was rapidly reversed during the transition to low irradiance. Despite the decline in P^{cell}_m, the cell-specific growth rate did not change significantly, and cellular chl concentrations slowly declined as cell abundance continued to increase. Although photoinhibition (β) was minimal, the flow of absorbed photons to photochemistry appears to have been significantly depressed throughout the entire observation period, resulting in slower acclimation to high irradiance in *F. cylindrus* #1102 than in *P. antarctica* #1871.

Higher P^{cell}_m when *F. cylindrus* #1102 was fully acclimated to 125 μmol photons · m^{-2} · s^{-1} suggests that a small increase in photosynthetic capacity (most likely in the form of increased $1/\tau$) eventually accompanies acclimation to high irradiance in *F. cylindrus* #1102, although a reduction σPSII certainly plays a larger role during the transition period. Reduced σPSII maintained by xanthophyll-cycle activity was also a prominent feature of cells fully acclimated to high irradiance. Immediately following the shift to low irradiance, DT · mol^{-1} chl and $\bar{a}^*$ declined, and Φ_M and F_v/F_m increased, producing a rise in α^{cell} and signifying an increase in σPSII. In response to the reduced irradiance, a significant increase in P^{cell}_m was also observed. However, the rise in P^{cell}_m was delayed 4 h until the xanthophyll cycle was fully deactivated and F_v/F_m had increased by 34%.

In contrast to *P. antarctica*, the physiological response of *F. cylindrus* #1102 shifted to low irradiance suggests that it tolerated rather than utilized high irradiance, relying upon reductions in σPSII and PSU · cell^{-1} to grow at 125 μmol photons · m^{-2} · s^{-1} rather than adding photosynthetic capacity by significantly increasing $1/\tau$. Trends observed during the shift to low irradiance in *F. cylindrus* #1102 are similar to those observed in Antarctica when natural assemblages of *Navicula glaceii* (Robinson et al. 1997) were transferred from surface water melt ponds (high light) to 4 μmol photons · m^{-2} · s^{-1} (low light). Under these conditions, P^{cell}_m rose after xanthophyll-cycle activity had relaxed and F_v/F_m and Φ_M began to recover. Furthermore, *P-E* coefficients, Φ_M, and F_v/F_m for surface assemblages were similar to those of *F. cylindrus* #1102 growing at 125 μmol photons · m^{-2} · s^{-1} and declined by a similar amount when shifted to low irradiance. *P-E* coefficients and C:chl in *F. cylindrus* #1102 cultures acclimated to 5 μmol photons · m^{-2} · s^{-1} were similar to those of natural diatom assemblages growing in low-irradiance under-ice habitats (Lizotte and Sullivan 1991).

Our data highlight the fact that *F. cylindrus* #1102 uses changes in xanthophyll-cycle activity and, hence, changes in σPSII, as a primary means to acclimate to changing irradiance. Similar mechanisms have been described in the diatom *Skeletonema costatum* (Falkowski and Owens 1980, Falkowski and LaRoche 1991). In addition, recent work showed that when *S. costatum* was shifted from 50 to 1,200 μmol photons · m^{-2} · s^{-1}, changes in xanthophyll-cycle content were large, while differences in P^{cell}_m were small (Anning et al. 2000), similar to our observations for *F. cylindrus* #1102. However, despite the importance of changing σPSII in *F. cylindrus* #1102, variation in functional PSU · cell^{-1} also appeared to play a role in acclimation to changing irradiance. Upon the shift to high irradiance, P^{cell}_mdeclined quickly, implying a decline in PSU · cell^{-1}. Given the rapid rise in F_v/F_m observed immediately after the shift to low irradiance, and the fast increase in P^{cell}_m that followed, it is unclear whether PSU · cell^{-1} actually changed significantly in *F. cylindrus* #1102 or whether simply functional PSU · cell^{-1} changed significantly when nonfunctional (or deactivated) photosystems that remained present were quickly repaired (or activated) when they became necessary. In contrast to *P. antarctica*, changes in $1/\tau$ appear to have only a minor effect on photosynthetic capacity *F. cylindrus* #1102.

Both *P. antarctica* #1871 and *F. cylindrus* #1102 generally acclimated more slowly to high irradiance than has been documented previously in temperate algal taxa. For example, rates of change in α^* in response to increasing irradiance for both *P. antarctica* #1871 and *F. cylindrus* #1102 (0.068 and 0.070 h^{-1}, respectively) were much lower than rates estimated by Cullen and Lewis (1988) when *Thalassiosira pseudonana* grown at 21°C was shifted from 20 to 100 μmol photons · m^{-2} · s^{-1} (0.72–1.84 h^{-1}). Rates of change in P^*_m were also slower in *P. antarctica* #1871 and *F. cylindrus* #1102 than those reported for *T. pseudonana* (Cullen and Lewis 1988). The slower acclimation rates are likely due in part to significantly lower specific growth rates related to the low temperature (Eppley 1972), as changes in cellular composition appear to be heavily influenced by the cell division rate. However, rates of change in α^* in both taxa were within the wide range of rates estimated in sea-ice diatoms (0.007–0.29 h^{-1}) shifted from an under-ice habitat to full sunlight (~1.5°C) and higher than rates of surface assemblages transferred to low irradiance (0.027–0.085 h^{-1}) (Lizotte and Sullivan 1991).

The physiological trends observed during the shift to low irradiance largely agree with previous studies. In both *F. cylindrus* #1102 and *P. antarctica* #1871, increased cell abundance drove a stoichiometric decline in chl · cell^{-1}, similar to previous findings for *Thalassiosira weissfloggi* (Post et al. 1984) and *Dunaliella tertiolecta* (Falkowski 1984). In *F. cylindrus* #1102, chl · cell^{-1} approximately doubled over the acclimation period, as was observed in *D. tertiolecta* (Sukenik et al. 1990), but increased much more

slowly than F_v/F_m, in agreement with findings in Antarctic cryptophytes (Buma et al. 1993) and *T. pseudonana* (Cullen and Lewis 1988). The most significant difference between our study and previous experiments examining photoacclimation to low irradiance was the high rate of cell division in *P. antarctica* #1871 after the transition to low irradiance, which outpaced chl production and resulted in unexpected declines in chl · cell^{-1}.

Significance for the Ross Sea. As both *P. antarctica* #1871 and *F. cylindrus* #1102 relied upon changes in σPSII to acclimate to changes in irradiance, two of the most prominent differences between taxa were the greater ability of *P. antarctica* #1871 to adjust photosynthetic capacity in response to changes in irradiance and the much longer time required to relax xanthophyll-cycle activity in *F. cylindrus* #1102. Surprisingly, our experimental results suggest that diatoms like *F. cylindrus* #1102 may dominate the shallow, high-light mixed layers of the Ross Sea not by acclimating rapidly, but conversely, because extensive photoprotection and slower rates of acclimation to changes in irradiance leave them less vulnerable to photoinhibition than rapidly acclimating taxa and allow them to survive in high-light environments that do not include a low-irradiance period in which repair can occur. Conversely, the faster rate at which *P. antarctica* #1871 adjusted its photosynthetic capacity to the ambient irradiance points to success in a deeply mixed irradiance regime.

In a deeply mixed water column, extensive photoprotection in surface waters and slow relaxation of the xanthophyll cycle would significantly reduce rates of CO_2 fixation in *F. cylindrus* #1102 relative to *P. antarctica* #1871, both at the sea surface and as cells mix deeper in the water column. Consequently, because it is able to quickly stop xanthophyll-cycle diversion of absorbed light energy away from photochemistry allowing for higher photosynthetic rates, *P. antarctica* #1871 would quickly outcompete *F. cylindrus* #1102 in a deeply mixed environment. However, *F. cylindrus* #1102 might be more successful in stable irradiance regimes, such as the constant low-irradiance environment of sea ice or the high-irradiance regime of a stratified, shallowly mixed water column. Under these conditions, *F. cylindrus* #1102 should outcompete a growth-prioritizing species like *P. antarctica*, which is more vulnerable to photodamage under high-light conditions without a deep enough mixing cycle to allow adequate time for photorepair and which may have higher respiratory costs under very low constant irradiance conditions.

Although recent work has shown that genetically distinct populations of a single diatom species can dominate the same location at different points in a seasonal cycle (Rynearson et al. 2006), similarities in the mechanisms of photoacclimation between *F. cylindrus* #1102 and other Antarctic sea-ice diatoms (Lizotte and Sullivan 1991, Robinson et al. 1997, Petrou et al. 2010) and between *P. antarctica* #1871 and other haptophytes (Dubinsky et al. 1986, Suggett et al. 2007) suggests that the two acclimation strategies we have identified may be broadly utilized by Southern Ocean populations of *P. antarctica* and ice-influenced diatom species. In addition, our findings suggest that the initial rates of acclimation of *P. antarctica* and *F. cylindrus*–like diatoms to springtime changes in irradiance are probably less important drivers of phytoplankton community composition in the Ross Sea than variability of the irradiance field.

We thank M. Palmer and G. Kulk for assistance in the laboratory. This research was funded by the Ocean Carbon Sequestration Research Program, Biological and Environmental Research (BER), U.S. Department of Energy (grant # DE-FG02-04ER63891 and # DE-FG02-04ER63861), and by a NASA Earth and Space Science Fellowship (# NNX07AO23H) awarded to L. Kropuenske.

Anning, T., MacIntyre, H. L., Pratt, S. M., Sammes, P. J., Gibb, S. & Geider, R. J. 2000. Photoacclimation in the marine diatom *Skeletonema costatum*. *Limnol. Oceanogr.* 45:1807–17.

Arrigo, K. R., DiTullio, G. R., Dunbar, R. B., Lizotte, M. P., Robinson, D. H., VanWoert, M. & Worthen, D. L. 2000. Phytoplankton taxonomic variability and nutrient utilization and primary production in the Ross Sea. *J. Geophys. Res.* 105:8827–46.

Arrigo, K. R., Mills, M. M., Kropuenske, L. R., Van Dijken, G. L., Alderkamp, A. C. & Robinson, D. H. 2010. Photophysiology in two major Southern Ocean phytoplankton taxa: productivity and growth of *Phaeocystis antarctica* and *Fragilariopsis cylindrus* under different irradiance levels. *Integr. Comp. Biol.* DOI: 10.1093/icb/icq021.

Arrigo, K. R., Robinson, D. H., Worthen, D. L., Dunbar, R. B., DiTullio, G. R., VanWoert, M. & Lizotte, M. P. 1999. Phytoplankton community structure and the drawdown of nutrients and CO_2 in the Southern Ocean. *Science* 283:365–7.

Arrigo, K. R., Weiss, A. M. & Smith, W. O. 1998. Physical forcing of phytoplankton dynamics in the western Ross Sea. *J. Geophys. Res.* 103:1007–21.

Buma, A. G. J., Noordeloos, A. A. M. & Larsen, J. 1993. Strategies and kinetics of photoacclimation in three Antarctic nanophytoflagellates. *J. Phycol.* 29:407–17.

Casper-Lindley, C. & Bjorkman, O. 1998. Fluorescence quenching in four unicellular algae with different light-harvesting and xanthophyll-cycle pigments. *Photosynth. Res.* 56:277–89.

Cota, G. F., Smith, W. O. & Mitchell, B. G. 1994. Photosynthesis of *Phaeocystis* in the Greenland Sea. *Limnol. Oceanogr.* 39:948–53.

Cullen, J. J. & Lewis, M. R. 1988. The kinetics of algal photoadaptation in the context of vertical mixing. *J. Plankton Res.* 10:1039–63.

DiTullio, G. R. & Smith, W. O. 1996. Spatial patterns in phytoplankton biomass and pigment distributions in the Ross Sea. *J. Geophys. Res.* 101:18467–77.

Dubinsky, Z., Falkowski, P. G. & Wyman, K. 1986. Light harvesting and utilization by phytoplankton. *Plant Cell Physiol.* 27:1335–49.

Dubinsky, Z. & Stambler, N. 2009. Photoacclimation processes in phytoplankton: mechanisms, consequences, and applications. *Aquat. Microb. Ecol.* 56:163–76.

Eppley, R. W. 1972. Temperature and phytoplankton growth in the sea. *Fish. Bull.* 70:1063–85.

Falkowski, P. G. 1983. Light–shade adaptation and vertical mixing of marine phytoplankton: a comparative field study. *J. Mar. Res.* 41:215–37.

Falkowski, P. G. 1984. Kinetics of adaptation to irradiance in *Dunaliella tertiolecta*. *Photosynthetica* 18:62–8.

Falkowski, P. G. & LaRoche, J. 1991. Acclimation to spectral irradiance in algae. *J. Phycol.* 27:8–14.

Falkowski, P. G. & Owens, T. G. 1980. Light-shade adaptation. *Plant Physiol.* 66:592–5.

Falkowski, P. G., Owens, T. G., Ley, A. C. & Mauzerall, D. C. 1981. Effects of growth irradiance levels on the ratio of reaction centers in two species of marine phytoplankton. *Plant Physiol.* 68:969–73.

Falkowski, P. G. & Raven, J. A. 2007. *Aquatic Photosynthesis.* 2nd ed. Princeton University Press, Princeton, New Jersey, 484 pp.

Geider, R. J. & MacIntyre, H. L. 2002. Physiology and biochemistry of photosynthesis and algal carbon acquisition. *In* Williams, P. J., Thomas, D. N. & Reynods, C. S. [Eds.] *Phytoplankton Productivity: Carbon Assimilation in Marine and Freshwater Ecosystems.* Blackwell, Oxford, UK, pp. 44–77.

Geider, R. J. & Platt, T. 1986. A mechanistic model of photoadaptation in microalgae. *Mar. Ecol. Prog. Ser.* 30:85–92.

Goffart, A., Catalano, G. & Hecq, J. H. 2000. Factors controlling the distribution of diatoms and *Phaeocystis* in the Ross Sea. *J. Mar. Syst.* 27:161–75.

Gowing, M. M., Garrison, D. L., Kunze, H. B. & Winchell, C. J. 2001. Biological components of Ross Sea short-term particle fluxes in the summer of 1995–1996. *Deep-Sea Res. Part I Oceanogr. Res. Pap.* 48:2645–71.

Hegseth, E. N. & von Quillfeldt, C. H. 2002. Low phytoplankton biomass and ice algal blooms in the Weddell Sea during the ice-filled summer of 1997. *Antarct. Sci.* 14:231–43.

Kang, S.-H. & Fryxell, G. A. 1992. *Fragilariopsis cylindrus* (Grunow) Krieger: the most abundant diatom in water column assemblages of Antarctic marginal ice-edge zones. *Polar Biol.* 12:609–27.

Kropuenske, L. R., Mills, M. M., van Dijken, G. L., Bailey, S., Robinson, D. H., Welschmeyer, N. A. & Arrigo, K. R. 2009. Photophysiology in two major Southern Ocean phytoplankton taxa: photoprotection in *Phaeocystis antarctica* and *Fragilariopsis cylindrus. Limnol. Oceanogr.* 54:1176–96.

Kudoh, S., Imura, S. & Kashino, Y. 2003. Xanthophyll-cycle of ice algae on the sea ice bottom in Saroma Ko lagoon, Hokkaido, Japan. *Polar Biosci.* 16:86–97.

Lavaud, J., Rousseau, B. & Etienne, A. L. 2004. General features of photoprotection by energy dissipation in planktonic diatoms (Bacillariophyceae). *J. Phycol.* 40:130–7.

Leonardos, N. 2008. Physiological steady state of phytoplankton in the field? An examples based on pigment profile of *Emiliania huxleyi* (Haptophyta) during a light shift. *Limnol. Oceanogr.* 53:306–11.

Leventer, A. & Dunbar, R. B. 1996. Factors influencing the distribution of diatoms and other algae in the Ross Sea. *J. Geophys. Res.* 101:18489–500.

Lizotte, M. P. & Sullivan, C. W. 1991. Rates of photoadaptation in sea ice diatoms from McMurdo Sound, Antarctica. *J. Phycol.* 27:367–73.

MacIntyre, H. L., Kana, T. M. & Geider, R. J. 2000. The effect of water motion on short-term rates of photosynthesis by marine phytoplankton. *Trends Plant Sci.* 5:12–7.

Melis, A., Murakami, A., Nemson, J. A., Aizawa, K., Ohki, K. & Fujita, Y. 1996. Chromatic regulation in *Chlamydomonas reinhardtii* alters photosystem stoichiometry and improves the quantum efficiency of photosynthesis. *Photosynth. Res.* 47:253–65.

Mills, M. M., Kropuenske, L. R., Van Dijken, G. L., Alderkamp, A.-C., Berg, G. M., Robinson, D. H., Welschmeyer, N. A. & Arrigo, K. R. 2010. Phytophysiology in two Southern Ocean phytoplankton taxa: photosynthesis of *Phaeocystis antarctica* (Prymnesiophyceae) and *Fragilariopsis cylindrus* (Bacillariophyceae) under simulated mixed-layer irradiance. *J. Phycol.* 46, DOI: 10.1111/j.1529-8817.2010.00923.x.

Mock, T. & Valentin, K. 2004. Photosynthesis and cold acclimation: molecular evidence from a polar diatom. *J. Phycol.* 40:732–41.

Moisan, T. A., Ellisman, M. H., Buitenhuys, C. W. & Sosinsky, G. E. 2006. Differences in chloroplast ultrastructure of *Phaeocystis antarctica* in low and high light. *Mar. Biol.* 149:1281–90.

Moisan, T. A. & Mitchell, B. G. 1999. Photophysiological acclimation of *Phaeocystis antarctica* Karsten under light limitation. *Limnol. Oceanogr.* 44:247–58.

Moisan, T. A., Olaizola, M. & Mitchell, B. G. 1998. Xanthophyll cycling in *Phaeocystis antarctica*: changes in cellular fluorescence. *Mar. Ecol. Prog. Ser.* 169:113–21.

Morel, F. M. M., Rueter, J. G., Anderson, D. M. & Guillard, R. R. L. 1979. Aquil: a chemically defined phytoplankton culture medium for trace metal studies. *J. Phycol.* 15:135–41.

Palmisano, A. C., SooHoo, J. B., SooHoo, S. L., Kottmeier, S. T., Craft, L. L. & Sullivan, C. W. 1986. Photoadaptation in *Phaeocystis pouchetii* advected beneath annual sea ice in McMurdo Sound, Antarctica. *J. Plankton Res.* 5:891–906.

Peloquin, J. A. & Smith, W. O. 2007. Phytoplankton blooms in the Ross Sea, Antarctica: interannual variability in magnitude, temporal patterns, and composition. *J. Geophys. Res* 112: CO8013, doi:10.1029/2006JC003816.

Petrou, K., Hill, R., Brown, C. M., Campbell, D. A., Doblin, M. A. & Ralph, P. J. 2010. Rapid photoprotection in sea-ice diatoms from the East Antarctic pack ice. *Limnol. Oceanogr.* 55:1400–7.

Pfannschmidt, T. 2005. Acclimation to varying light qualities: towards the functional relationship of state transitions and adjustment of photosystem stoichiometry. *J. Phycol.* 41:723–5.

Post, A. F., Dubinsky, Z., Wyman, K. & Falkowski, P. G. 1984. Kinetics of light-intensity adaptation in a marine planktonic diatom. *Mar. Biol.* 83:231–8.

Price, N. M., Harrison, G. I., Hering, J. G., Hudson, R. J., Nirel, P. M. V., Palenik, B. & Morel, F. M. M. 1989. Preparation and chemistry of the artificial algal culture medium Aquil. *Biol. Oceanogr.* 6:443–61.

Rivkin, R. B., Seliger, H. H., Swift, E. & Biggley, W. H. 1982. Light-shade adaptation by the oceanic dinoflagellates *Pyrocystis noctiluca* and *P. fusiformis. Mar. Biol.* 68:181–91.

Robinson, D. H., Kolber, Z. & Sullivan, C. W. 1997. Photophysiology and photoacclimation in surface sea ice algae from McMurdo Sound, Antarctica. *Mar. Ecol. Prog. Ser.* 147:243–56.

Rynearson, T. A., Newton, J. A. & Armbrust, E. V. 2006. Spring bloom development, genetic variation, and population succession in the planktonic diatom *Ditylum brightwellii. Limnol. Oceanogr.* 51:1249–61.

Schoemann, V., Becquevort, S., Stefels, J., Rousseau, V. & Lancelot, C. 2005. *Phaeocystis* blooms in the global ocean and their controlling mechanisms: a review. *J. Sea Res.* 53:43–66.

Smith, W. O., Nelson, D. M., DiTullio, G. R. & Leventer, A. R. 1996. Temporal and spatial patterns in the Ross Sea: phytoplankton biomass, elemental composition, productivity and growth rates. *J. Geophys. Res.* 101:18455–65.

Smith, W. O., Shields, A., Peloquin, J., Catalano, G., Tozzi, S., Dinniman, M. & Asper, V. 2006. Interannual variations in nutrients, net community production, and biogeochemical cycles in the Ross Sea. *Deep-Sea Res. Part II Top. Stud. Oceanogr.* 53:815–33.

Suggett, D. J., Le Floc'H, E., Harris, G. N., Leonardos, N. & Geider, R. J. 2007. Different strategies of photoacclimation by two strains of *Emiliania huxleyi* (Haptophyta). *J. Phycol.* 43:1209–22.

Sukenik, A., Bennett, J. & Falkowski, P. G. 1987. Light saturated photosynthesis limitation by electron transport or carbon fixation? *Biochim. Biophys. Acta* 891:205–15.

Sukenik, A., Bennett, J., Mortain-Bertrand, A. & Falkowski, P. G. 1990. Adaptation of the photosynthetic apparatus to irradiance in *Dunaliella tertiolecta. Plant Physiol.* 92:891–8.

Tortell, P. D., Payne, C., Geugen, C., Strzepek, R. F., Boyd, P. W. & Rost, B. 2008. Inorganic carbon uptake by Southern Ocean phytoplankton. *Limnol. Oceanogr.* 53:1266–78.

Van Hilst, C. M. & Smith, W. O. 2002. Photosynthesis/irradiance relationships in the Ross Sea, Antarctica, and their control by phytoplankton assemblage composition and environmental factors. *Mar. Ecol. Prog. Ser.* 226:1–12.

Wright, S. W. & van den Enden, R. L. 2000. Phytoplankton community structure and stocks in the East Antarctic marginal ice zone (BROKE survey, January–March 1996) determined by CHEMTAX analysis of HPLC pigment signatures. *Deep-Sea Res. Part II Top. Stud. Oceanogr.* 47:2363–400.